UC Davis
UC Davis Previously Published Works

## Title
Cyclic Loading Response of Silt with Multiple Loading Events

## Permalink
https://escholarship.org/uc/item/11h4p0t4

## Journal
Journal of Geotechnical and Geoenvironmental Engineering, 143(10)

## ISSN
1090-0241

## Authors
Price, AB
DeJong, JT
Boulanger, RW

## Publication Date
2017-10-01

## DOI
10.1061/(asce)gt.1943-5606.0001759

Peer reviewed

eScholarship.org Powered by the California Digital Library
University of California

# Cyclic Loading Response of Silt with Multiple Loading Events

A. B. Price[1], J. T. DeJong[2], and R. W. Boulanger[3]

[1]Corresponding Author, Ph. D. Candidate, Department of Civil and Environmental Engineering, University of California, Davis, CA, USA, abprice@ucdavis.edu

[2]Professor, Department of Civil and Environmental Engineering, University of California, Davis, CA, USA

[3]Professor, Department of Civil and Environmental Engineering, University of California, Davis, CA, USA

## Abstract

The evolution of cyclic resistance with multiple loading events is evaluated for non-plastic and low plasticity silts with plasticity indices of 0 and 6 respectively. A series of direct simple shear tests with multiple cyclic loading and reconsolidation stages is performed on young, slurry sedimented specimens. Evolution of cyclic strength with a series of multiple loading events is examined with respect to densification from post cyclic reconsolidation, shear strain induced fabric, and initial consolidation history. Initially normally consolidated specimens of both silts are shown to develop progressive increases in cyclic strength with prior strain history, with cyclic resistance ratios ultimately exceeding 0.6. Specimens consolidated with an initial overconsolidation ratio of 2 experience an 18%-32% loss of cyclic strength following the first stage of cyclic shearing and reconsolidation. The two silts develop similar magnitudes of reconsolidation strain, but the low plasticity silt is shown to require more volumetric strain (and therefore more loading events) to develop large cyclic strengths. Implications for future advances in liquefaction triggering correlations and engineering practice are discussed.

## Introduction

Strain history developed from earthquake induced cyclic loading appears capable of either increasing or decreasing cyclic resistance for future shaking events, depending on the number and nature of the past shaking events and the characteristics of the soil deposit. Empirical field evidence of recurrent liquefaction (e.g., recent observations in Japan and New Zealand by Wakamatsu 2012 and Maurer et al. 2014) suggests that cyclic resistance may increase or decrease following a single shaking event, whereas the in-situ strengthening over geologic time for deposits in seismically active regions suggests cyclic resistance is likely to increase over a series of multiple events. Case history based liquefaction triggering correlations using cone penetration test (CPT) and standard penetration test (SPT) data are assumed to implicitly account for the effect of prior strain history through its effects on both cyclic strength and penetration resistance; such methods are generally assumed applicable in forward applications regardless of prior strain history. A fundamental understanding of the effects of prior strain history on cyclic resistance and in-situ penetration resistance across multiple shaking events is necessary for improved interpretations of case history data and inclusion of such effects, if appropriate, in liquefaction triggering correlations.

The effect of prior earthquake shaking on the cyclic resistance of non-plastic soils is thought to be primarily dependent on: (1) destruction of any structure developed from ageing, biogeochemical processes, and prior loading history, (2) changes in density from post-cyclic reconsolidation, (3) post-cyclic aging, and (4) evolving anisotropy/structure (Olson et al. 2001, Oda et al. 2001). Early studies evaluating the effect of strain history on cyclic resistance have focused on the influence of single preshearing events on young, reconstituted clean sands. There is consensus in the literature that the effect of preshearing (monotonic or cyclic) is strain dependent. Increased cyclic resistance following small amplitude undrained cyclic or monotonic preshearing and subsequent reconsolidation have been observed by several groups of researchers (e.g., Finn et al. 1970, Seed et al. 1977, Ishihara and Okada 1978, Oda et al. 2001). Finn et al. (1970) suggested increases in lateral earth pressures and minor adjustments at sand grain contacts could be responsible for increases in resistance following small strain cyclic loading. Seed et al. (1977) observed similar increases in liquefaction resistance following a series of small shaking events (generating excess pore pressure ratios less than 30%) in 1-g shaking table tests on sand. They attributed this strength increase to changes in particle structure that decreased the contractive tendency of the sand (while the relative density remained practically unchanged). Conversely, large strain preshearing (generally shear strains exceeding 1%) has been shown to reduce cyclic resistance (Oda et al. 2001, Suzuki and Toki 1984, Ishihara and Okada 1978). Oda et al. (2001) attributed decreases in cyclic resistance following large strain preshearing to induced anisotropy of a column like structure. Ishihara and Okada (1978) and Suzuki and Toki (1984) both observed cyclic resistance following large strain preshearing to be dependent on the directionality (triaxial compression vs. extension) of both the final cycle of preshearing prior to reconsolidation and the first quarter cycle of subsequent cyclic shearing. These experimental studies on young, uncemented sands generally attribute changes in cyclic resistance following preshearing to changes in soil fabric or the arrangement of soil particles (Mitchell and Soga 2005). The effect of post-liquefaction ageing was evaluated by Maurer et al. (2014) using empirical observations from the Canterbury earthquake sequence in Christchurch, New Zealand. They attributed reduced cyclic resistance following liquefaction to loss of ageing effects. Collectively, it is clear from these studies and others that the effect of single preshearing events on the cyclic resistance of sand is multifaceted; it is dependent on preshearing strain magnitude, loading directionality, and ageing effects as well as a variety of additional complexities encountered in natural deposits including cementation, biogeochemical processes, and variable loading and consolidation histories.

Multiple shaking events have generally been shown to produce cumulative increases in resistance (e.g., Ha et al. 2011, El-Sekelly et al. 2016, Darby et al. 2016), even though single preshearing events may improve or reduce the cyclic resistance of sands. Ha et al. (2011) observed an initial reduction followed by an increase in liquefaction resistance in a series of 1-g shaking table tests on five Korean sands. El-Sekelly et al. (2016) performed a 25-g centrifuge test with silty sand subjected to a series of shaking events based on seismic records from the Wildlife Liquefaction Array research site located near the southern reach of the San Andreas Fault system in California. The shaking sequence used in their study consisted of repeated application of one large magnitude shaking event followed by ten small magnitude events. They observed the following: (1) an increase in liquefaction resistance from each consecutive small magnitude event, (2) a decrease in liquefaction resistance for small magnitude events following a large magnitude event, and (3) a general increase in liquefaction resistance across the total 66 shakes applied, which was conceptually consistent with empirical evidence of increased resistance of the Wildlife array site over time. Darby et al. (2016) performed an 80-g centrifuge test on Ottawa sand subjected to a series of shaking events of ramping intensity and observed progressive increases in both liquefaction resistance and cone penetration resistance.

The body of laboratory element and physical model test data for non-plastic and low plasticity silts is much less developed than for sands. Laboratory studies have shown the cyclic strength of non-plastic and low-plasticity silts to depend on the plasticity (or percentage of plastic fines), the failure criteria, and the basis for comparing results across soils, such as for the same depositional method, same void ratio, same overconsolidation ratio, or same penetration resistance (e.g., Romero 1995, Guo and Prakash 1999, Bray and Sancio 2006, Sanin and Wijewickreme 2006, Kokusho et al. 2012, Wijewickreme and Soysa 2016). Non-plastic and low plasticity silts are also not well represented in the case history database used for development of empirical procedures for liquefaction triggering (for sand-like soils) or cyclic softening (for clay-like soils) (Boulanger and Idriss 2016). The evolution of cyclic strength for these soil types with prior cyclic loading or recurrent liquefaction has not been established.

The purpose of this paper is to evaluate the evolution of cyclic resistance with multiple cyclic loading and reconsolidation stages for a non-plastic silt with a plasticity index (PI) of 0 and a low plasticity, PI = 6 silt. A series of direct simple shear (DSS) tests was employed to track the evolution of behavior from a loose slurry deposited condition to specimens densified by multiple cyclic shearing and reconsolidation stages with cyclic resistance ratios (CRRs) exceeding 0.6. While numerous aspects of soil behavior conceivably contribute to the progression of cyclic resistance with prior strain history for natural soils in situ, this study focuses on the evolution of cyclic strength resulting from: (1) densification from post cyclic reconsolidation, (2) shear strain induced fabric evolution, and (3) initial consolidation history. This study was limited to young, slurry sedimented soils with little ageing allowed between cyclic loading events. Stage-specific and cumulative changes in cyclic resistance resulting from series of multiple cyclic loading events are presented and discussed. Finally, the implications for future advances in liquefaction triggering correlations and engineering practice are discussed.

## Methods and Materials

The effect of recurrent liquefaction events on cyclic strength is conceptually illustrated in Fig. 1. A soil element within a liquefiable layer (Fig. 1a) is shaken by a series of hypothetical earthquake events. Prior to any shaking, the element exists at state #1 in the void ratio-vertical effective stress space (Fig. 1b). Earthquake induced cyclic loading (EQ #1) liquefies the soil element as portrayed by the leftward path extending from state #1. Following shaking, reconsolidation densifies the soil element to state #2 assuming unimpeded pore pressure dissipation in the soil profile. A second earthquake (EQ #2) re-liquefies the soil element, which subsequently reconsolidates to state #3. Ensuing earthquake events continue to liquefy the soil element, each followed by reconsolidation and associated densification. The effect of this hypothetical loading history (cycles of earthquake induced cyclic loading followed by reconsolidation) is a progressive increase in both cyclic strength and indices of density as conceptualized in Fig. 1c. The laboratory testing methods described herein aim towards mimicking this hypothetical loading history.

Direct simple shear tests with multiple cyclic shearing and reconsolidation stages were performed to evaluate the evolution of cyclic strength with prior strain history. DSS testing was performed using a GEOTAC DigiShear NGI-type DSS device (Bjerrum and Landva 1966); stacked rings enclosing a latex membrane were used to prevent radial deformations. Specimen diameter was 66.72 mm and specimen heights ranged from about 11.7-16.2 mm. The resulting diameter to height ratios (of about 4.1-5.7) are thought to be sufficient for engineering purposes to prevent any significant effect from the lack of complementary shear stresses given both DSS testing standards (ASTM D6528-07) and the body of literature examining such effects (e.g., Franke et al. 1979). Any effect on the cyclic response resulting from the lack of complementary shear stresses is expected to diminish as DSS tests with multiple cyclic shearing and reconsolidation stages progress and specimen diameter to height ratios increase. DSS specimens were initially consolidated to a vertical effective consolidation stress, $\sigma'_{vc}$, of 100 kPa by constant rate of stress loading (about 100kPa/hr). Specimens were aged roughly 16 hours following the end of primary consolidation. Undrained stress controlled cyclic shearing at a strain rate of 5%/hr was performed until the development of 3% single amplitude shear strain. Following each cyclic shearing stage, specimens were re-centered to the horizontal position realized at the end of initial consolidation under undrained conditions. Reconsolidation to $\sigma'_{vc}$ = 100 kPa was then performed with constant rate of stress loading (about 100kPa/hr). During reconsolidation the shear stress was maintained at 0 kPa. To limit shear strain development during reconsolidation, sufficient vertical stress (about 8.5 kPa) was allowed to develop prior to shear stress zeroing. Specimens were aged for 1 hour after reconsolidation, before the next stage of cyclic loading. This sequence of cyclic loading, re-centering, and reconsolidation was repeated with a stepwise ramping of the cyclic stress ratio (CSR) targeting development of 3% single amplitude shear strain in close to 15 cycles. A given CSR was applied for consecutive cyclic shearing stages until greater than 15 cycles was required to develop 3% shear strain. The CSR was then increased such that 3% shear strain was achieved in significantly less than 15 cycles during the next cyclic shearing stage. The described DSS test methodology featuring multiple cyclic shearing and reconsolidation stages is referred to as DSScsh testing (DSS testing with cyclic strain history) herein.

Laboratory testing was performed for slurry deposited specimens of non-plastic, PI = 0 and low plasticity, PI = 6 silt. The PI = 0 silt (also referred to as 100S) was 100% crushed, highly angular silica silt (SIL-CO-SIL 250) with a median particle size of about 50 microns. The PI = 6 silt (also referred to as 80S20K) was a mixture of the non-plastic, PI = 0 silt (80% by dry mass) and kaolin clay (20% by dry mass, Old Hickory No. 1 Glaze). Slurries were mixed under vacuum by a propeller mixing blade and mechanical rotation of a cylindrical mixing chamber. The slurry deposition method used in this study is capable of producing specimens ranging from the non-plastic, PI = 0 silt to highly plastic clays while maintaining uniform mixtures of binary constituents. The slurry deposition method was selected to provide common laboratory preparation of specimens of the PI = 0 silt and PI = 6 silt with initial fabric analogous to that found in fluvial depositional environments. The PI = 0 silt was deposited at a water content of 29.6% and the PI = 6 silt was deposited at a water content of 44.6%, twice its liquid limit. Following deposition into DSS molds, specimens were allowed to consolidate under their self-weight prior to placement of the DSS top cap. This was done to prevent the slurry from flowing around the edge of the top cap during placement. Once mounted onto the DSS frame and normally consolidated to $\sigma'_{vc}$ = 100 kPa the PI = 0 and 6 silts had initial void ratios of about 0.61 and 0.63, respectively. At a normally consolidated, $\sigma'_{vc}$ = 100 kPa condition the PI = 0 silt was slightly dense of critical state while the PI = 6 silt was loose of critical state. This difference in initial states and its consequence for the monotonic shearing behavior of the two silts is discussed in the following section.

## Monotonic and Cyclic Behaviors for Virgin PI = 0 and 6 Silt Specimens

One dimensional compression and monotonic undrained DSS tests were performed on virgin specimens of the PI = 0 and PI = 6 silts. The term virgin is used herein to describe specimens that have never been cyclically sheared. Results from one dimensional compression tests carried out to $\sigma'_v$ =100 MPa are shown in Fig. 2. The shape of the compression curve for the PI = 0 silt specimen is typical of non-plastic soils; the response was initially stiff followed by increased compressibility consistent with increasing amounts of particle/asperity crushing as the vertical stress exceeded about 30 MPa. The PI = 6 silt was much more compressible in one-dimensional compression than the PI = 0 silt for stresses less than about 20 MPa (Fig. 2). Undrained monotonic DSS responses for virgin normally consolidated PI = 0 and PI = 6 silt specimens for a range of initial confinements are shown in Fig. 3. The PI = 0 silt was dilative at large shear strains (i.e., stress paths extend to the right) indicating the specimens were dense of critical state for the initial conditions tested. The PI = 6 silt was contractive (i.e., stress paths extend to the left) indicating the specimens were loose of critical state for the initial conditions tested. In addition, the PI = 6 silt showed undrained strength normalization across the range of initial conditions tested. The measured undrained strength ratio, $s_u/\sigma'_{vc}$, for the PI = 6 silt was 0.16; this strength is less than the empirical average undrained strength ratio, $s_u/\sigma'_{vc} = 0.22$, typical for sedimentary clays which may partly reflect the young age of the specimens used in this study.

Cyclic strengths for virgin normally consolidated slurry deposited specimens of the two silts were similar. Cyclic strengths were measured by stress controlled undrained DSS tests on slurry deposited specimens. Cyclic strengths defined for a failure criterion of 3% single amplitude shear strain for virgin specimens with overconsolidation ratios (OCRs) of 1, 2, and 4 are shown in Fig. 4; OCR = $\sigma'_{vp} / \sigma'_{vc}$ where $\sigma'_{vp}$ = preconsolidation stress. A failure criterion of 3% shear strain was chosen because it closely coincides with development of an excess pore pressure ratio $r_u = \Delta u/\sigma'_{vc} = 100\%$ for cyclic tests without a shear stress bias (e.g., Ishihara and Yoshimine 1992) and the development of limiting $r_u$ values with a shear stress bias (Boulanger and Seed 1995). The sensitivity of cyclic strength to failure criterion is discussed later. Each point in Fig. 4a represents the measured response from a single undrained cyclic DSS test; stress-strain responses for individual tests are discussed in the following sections. The trend lines in Fig. 4a are power expressions of the form CRR = $a \cdot N^{-b}$ where the CRR is the cyclic resistance ratio, N is the number of cycles to failure, and a and b are fitting parameters. The parameter b, which describes the slope of the fitted relationships, was set independent of OCR based on two considerations: (1) the OCR = 1 datasets better constrained the regressions especially at values of N>15 and (2) the improvement of fit with b values dependent on OCR was minimal (e.g., $R^2$ values). Fig 4b shows the increase in cyclic strength defined for 3% single amplitude shear stain in 15 cycles versus OCR. The strength increase with OCR was greater for the PI = 6 silt than for the PI = 0 silt, which may reflect the greater compressibility of the PI = 6 silt.

## Cyclic Strength Evolution with Prior Strain History for PI = 0 Silt

### *Initially Normally Consolidated Specimens*

The evolution of the cyclic strength of specimens of initially normally consolidated PI = 0 silt with prior strain history was evaluated using DSScsh tests with multiple cyclic shearing and reconsolidation stages. A summary in e-$\sigma'_v$ stress space for a DSScsh test on an initially normally consolidated PI = 0 silt specimen is shown in Fig. 5. The slurry deposited silt specimen was initially normally consolidated to $\sigma'_v$ = 100 kPa (state A1). The specimen was subjected to thirteen cyclic shearing stages, each of which was followed by reconsolidation to $\sigma'_v$ = 100 kPa (except for the final shearing stage). CSRs of approximately 0.13 (states A1-A4), 0.21 (B1-B4), 0.41 (C1-C3), and 0.59 (D1-D2) were applied. Specimen states and cyclic shearing stages are denoted using an alphanumeric nomenclature; the letter corresponds to the applied CSR value and the number specifies the stage count at a given CSR. Stress-strain responses and stress paths for the labeled shearing stages in Fig. 5 (A1, A4, B3, and C2) are discussed later in this section. Post-cyclic reconsolidation strains were about 1.5% to 0.3% per stage, generally decreasing with increased density. All strains presented herein were computed from specimen heights updated at the start of each shearing stage. The measured reconsolidation strains for these silts are similar to those for sands for 3% maximum single amplitude shear strain (e.g., Ishihara 1993) and less than the 2.5-4.5% measured by Sanin and Wijewickreme (2006) for specimens of Fraser River silt (PI = 4) that generated max $r_u$ values close to 100%.

The evolution of the cyclic resistance of initially normally consolidated PI = 0 silt specimens with strain history during DSScsh testing appears to be principally controlled by changes in dilatancy resulting from post-cyclic densification. Cyclic shearing and reconsolidation responses for states A1, A4, B3, and C2 for the DSScsh test summarized in Fig. 5 are shown in Fig. 6. The first cyclic shearing stage shown (stage A1) is the virgin slurry deposited response. The next three stages plotted (A4, B3, and C2) each developed 3% shear strain in close to 15 cycles for different magnitudes of loading. As the density of the specimen increased, greater CSRs were required to reach 3% shear stain in close to 15 cycles. Comparison of the cyclic shearing responses of states A1 and C2 illustrates the primary behaviors associated with the observed increases in cyclic resistance with prior strain history. All cyclic shearing responses exhibit incremental accumulation of shear strains with each loading cycle, or "cyclic mobility" behavior (Castro 1975), with the rate of strain accumulation progressively decreasing with increasing specimen density. Shearing stage A1 accumulated small shear strains until the excess pore pressure ratio ($r_u$) exceeded about 90% at which point large shear strains developed in just a couple of cycles. Conversely, stage C2 developed near 1% shear strain during the first ¼ cycle of loading but more gradually accumulated large shear strains at high values of $r_u$. The slower rate of shear strain accumulation exhibited by stage C2 (and subsequent stages) is attributed to its increased dilative tendency during undrained shearing to large strains. The relative dilative tendencies of the four responses in Fig. 6 can be inferred from the slopes of the normalized vertical effective stress vs. shear strain curves; a progressive increase in dilatancy developed throughout the test because of densification from accumulated post-cyclic reconsolidation strains. The cyclic resistance is insensitive to the failure strain criteria for states exhibiting rapid development of large shear strains at high values of $r_u$ (e.g., state A1), and hence the cyclic resistance is essentially controlled by the rate of pore pressure generation. In contrast, the cyclic resistance becomes more sensitive to the failure strain criteria for denser states exhibiting a slower rate of strain accumulation per loading cycle. In addition, the cyclic resistance for the latter denser states starts to exhibit dependence on the initial stiffness and associated strain development in the first ¼ to ¾ cycles. The evolution of cyclic resistance with prior strain history therefore reflects the progressive increase in resistance to shear strain accumulation (i.e., smaller increments of shear strain per loading cycle) and the failure strain criterion.

To compare behaviors across the multiple stages of cyclic loading applied during a DSScsh test, the measured number of cycles to a given failure criterion (e.g., 3% single amplitude shear strain) at the applied CSR for each shearing stage was projected to a cyclic resistance ratio (CRR) for 15 cycles. This projection is illustrated in Fig. 7. The measured stress-strain response for stage B4 is shown in Fig. 7a for the same DSScsh test shown in Figs. 5 and 6. The applied CSR (0.21) and measured number of cycles to 3% single amplitude shear strain (18.5) are plotted in Fig. 7b. The cyclic strength projection from the measured number of cycles to 15 cycles is dependent on the slope of the assumed CSR-N relationship. The CSR-N trend for tests on virgin silt specimens (from Fig. 4) is plotted in Fig. 7b. The slope (parameter b) of this fit could be applied to compute projected CRR values for 15 cycles from the measured data for stage B4, however, parameter b is known to increase with soil dilatancy (or CRR). Fig. 7c shows the variation of parameter b with CRR assumed by Boulanger and Idriss (2014) in the development of their magnitude scaling factor which was based on laboratory data for soils with a wide range of fines contents and plasticity indices. The single data point for the virgin normally consolidated silt is in good agreement with this relationship. The cyclic test data for overconsolidated specimens (Fig. 4) did not exhibit the trend of this relationship, which suggests the effects of OCR and densification on b values are not equally represented by changes in CRR values. Nonetheless, the relationship was slightly shifted to match the measured b values for virgin normally consolidated specimens, and then used in an iterative procedure to compute b and CRR values for each DSScsh test stage. For virgin overconsolidated shearing stages, strengths were projected using the measured b values (Fig 4) rather than those predicted by the adopted CRR-b relationship. The assumed fit and projected CRR value for stage B4 is shown in Fig. 7b and the projection of every stage from this DSScsh test and corresponding b values are shown in Figs. 7c and 7d. The increase in slope with cyclic strength is evident in the assumed fits in Fig. 7d. The described cyclic strength projection provides a rational way to compare responses of each stage of a given DSScsh test while honoring both the measured data for virgin specimens and the body of data in the literature. Potential errors associated with the projection of cyclic strengths are minimized by only using responses for which the given failure criterion developed between 4 and 30 cycles of loading (unless otherwise indicated). As a result, not all consecutive stages of a given DSScsh test are depicted in the summary plots presented herein. Alternative models for specifying b and its variation with loading history were evaluated, but the results and trends were insensitive to alternative models because the projections were not extending over a large number of loading cycles. The slight strength decrease from stage A1 to A2 evident in Fig. 7d is partly attributed to differences in secondary compression time and is conceptually consistent with age effects on liquefaction resistance in sands (e.g., Maurer et al. 2014, Hayati and Andrus 2009). Ageing effects from the 16 hours of secondary compression following virgin consolidation (prior to shearing A1) provided a greater strength increase than the combined effects of about 1.5% reconsolidation strain and 1 hour of secondary compression time (following shearing of A1) assuming the effects of fabric evolution from prior cyclic shearing on cyclic strength were of secondary order.

Projected CRRs for 15 cycles are plotted versus void ratio (e) in Fig. 8 for two DSScsh tests on initially normally consolidated PI = 0 silt specimens. The test results are plotted for both 3% single amplitude and 5% double amplitude shear strain failure criterion. A double amplitude failure criterion was used to evaluate any potential bias in the computed strengths from the directionality of the stress-strain responses; the choice of failure criterion was not important for the early stages of loading, but became more significant as the specimens became denser and the responses were governed by slower rates of shear strain accumulation. Stress-strain responses for later stages of cyclic shearing generally developed greater shear strains in the direction that the previous shearing stage was stopped prior to its re-centering and reconsolidation; this directional dependency is consistent with the observations made by Ishihara and Okada (1978) and Suzuki and Toki (1984) previously discussed. For example, shearing stages B3 and C2 in Fig. 6 exhibit a bias towards the negative shear strain direction (much of which is established in the first cycle of shearing), whereas other cyclic shearing stages developed bias towards the positive direction. The two tests show reasonable agreement demonstrating test repeatability. The curvature of the derived relationships transitions from relatively flat at looser states (void ratios greater than about 0.55) to steep at denser states (void ratios smaller than about 0.47) as the behavior evolves from being characterized by the rapid development of large shear strains at high $r_u$ values (e.g., state A1 in Fig. 6) to being controlled by slow strain accumulation by cyclic mobility (e.g., state C2 in Fig. 6). Likewise, the sensitivity of cyclic strength to failure criterion transitions with the dominant mechanism of large shear strain development. The responses on the flat part of the CRR-e curve, referred to as "loose" herein, were generally insensitive to failure criterion. The shearing response for state C2 in Fig. 6 illustrates the increased sensitivity to failure criterion exhibited by denser states, referred to as "dense" herein; significantly different numbers of cycles were required to develop $r_u$ = 90%, 1% shear strain, and 3% shear strain. This sensitivity to failure criteria is consistent with triaxial test results on sand at different relative densities (e.g., Ishihara and Yoshimine 1992). In general, the strength increase from any one cyclic shearing and reconsolidation sequence was relatively modest, especially for "loose" states with cyclic resistance ratios less than about 0.25; however, the full series of multiple shearing and reconsolidation stages cumulatively increased the cyclic strength significantly.

Three factors that influenced, or may have influenced, the evolution of responses and cyclic strengths in DSScsh tests on initially normally consolidated specimens of the PI = 0 silt are: (1) densification from accumulation of reconsolidation strains, (2) fabric induced by the loading history, and (3) potential non-uniformity of densities within the specimen. If a non-uniform density distribution develops during a DSScsh test, it is suspected that the measured response will be weaker than for a uniform specimen at the same global void ratio because shear strains may become concentrated in looser regions of the specimen depending on the nature of the non-uniformity. Densification and the associated increase in large strain dilatancy was the primary mechanism by which cyclic strength (for a failure criterion of 3% shear strain) increased throughout DSScsh tests on initially normally consolidated specimens of the PI = 0 silt. Evidence of strain-induced fabric was observed for repeated cyclic loadings at the same CSR. Stress-strain curves and stress paths are shown in Fig. 9 for four consecutive cyclic shearing stages at the same CSR (stages B1, B2, B3, and B4 for the DSScsh test shown in Figs. 5-7). B1 was the first cyclic shearing stage with a CSR = 0.21 in this DSScsh test. Subsequent loadings at the same CSR (stages B2, B3, and B4) show nearly identical stress paths and stress-strain responses for the first five cycles of loading. Similarity of these responses is also evident in Figs. 9c and 9d showing maximum shear strain and maximum excess pore pressure ratio versus cycle number. After about the 5$^{th}$ shearing cycle, the responses begin to deviate with later stages of loading generating excess pore pressures and shear strains more slowly; this may be attributable to increases in dilatancy from densification effecting the responses more significantly than residual fabric from prior loading stages once large enough shear strains develop in the specimen. While the effects of fabric evolution cannot be fully decoupled from the effects of densification for the DSScsh tests performed in this study, it is reasonable that the memory of prior loading can initially weaken the response of consecutive loadings at similar CSRs. This can be inferred from the relatively constant initial rates of pore pressure generation evident in the responses of stages B2, B3 and B4, despite their differences in density. Decreasing rates of pore pressure generation with increasing density would be expected if there was no effect from fabric evolved during prior loading history. It is hypothesized that subsequent loadings at significantly larger CSRs would be less affected by the fabric developed from consecutive loadings at smaller CSRs; this hypothesis is consistent with the centrifuge test based findings of El-Sekelly et al. (2016).

### *Initially Overconsolidated Specimens*

The influence of initial consolidation history on the evolution of cyclic strength with prior strain history for the PI = 0 silt was evaluated using DSScsh tests on initially overconsolidated specimens. The cyclic strengths (for 3% single amplitude shear strain in 15 cycles) of virgin specimens with OCRs of 2 and 4 were about 1.5 to 2 times the strength of normally consolidated virgin specimens (see Fig 4b). This strength increase is attributed to the combined effects of densification, fabric, and increases in horizontal stress induced by overconsolidation. Volumetric strains, relative to a $\sigma'_{vc}$ = 100 kPa $K_0$ normally consolidated reference stress, of about 0.5% to 1% developed during overconsolidation to an OCR = 2. The densification from overconsolidation to an OCR = 2 was less than that from reconsolidation following the first several stages of cyclic shearing during DSScsh tests on initially normally consolidated PI = 0 silt specimens (about 1.5% volumetric strain per reconsolidation stage). The strength gain from overconsolidation (to an OCR = 2) arising from densification appears to be secondary to fabric and lateral stress effects given: (1) the relative compressibility during overconsolidation and reconsolidation, (2) the marginal strength increase with decreasing void ratios measured during the first several cyclic shearing stages for DSScsh tests on initially normally consolidated specimens (flat part of curve in Fig. 8), and (3) the strength changes associated with the fabric evolved from cyclic shearing are secondary to those from densification for DSScsh tests on initially normally consolidated specimens. The progression of cyclic strength and shearing response following cyclic shearing and reconsolidation of initially overconsolidated specimens of the PI = 0 silt is presented below.

The fabric and lateral stresses developed from overconsolidation of the PI = 0 silt appeared to have been functionally erased by subsequent stages of cyclic shearing and reconsolidation. Responses for consecutive cyclic shearing stages at a CSR of about 0.15 from a DSScsh test on an initially overconsolidated (OCR = 2) PI = 0 silt specimen are shown in Fig. 10. Stress-strain responses and stress paths for the first two cyclic loading stages are shown in Figs. 10a and 10b. Maximum shear strain and excess pore pressure ratio are plotted versus cycle number for the first four cyclic loading stages in Figs. 10c and 10d; circles are plotted at a maximum excess pore pressure ratio of 75% for reference purposes. The virgin response of the overconsolidated specimen was initially stiff with slow generation of excess pore pressure. Once the $r_u$ exceeds about 75% large shear strains developed in just a couple of cycles similarly to the virgin response of normally consolidated specimens. Comparable rates of large strain accumulation at high values of $r_u$ for virgin overconsolidated and normally consolidated specimens is reasonable given their similar densities and the flat curvature of the CRR-e relationships derived from tests on initially normally consolidated specimens for "loose" states. The slow initial rate of excess pore pressure generation evident in the virgin overconsolidated response is attributed to the fabric and lateral stresses developed during overconsolidation. The second, third and fourth stages of cyclic loading exhibit significantly faster excess pore pressure generation implying that the fabric developed during overconsolidation is mostly erased by the development of large shear strains during cyclic shearing and subsequent reconsolidation. The virgin overconsolidated response required greater energy (a greater number of cycles and hysteretic work) to develop large shear strains than the three ensuing responses; additional energy was needed to break down the fabric induced by overconsolidation and generate high values of $r_u$. However, all four shearing stages generated $r_u$ values of 75% at about 1% shear strain suggesting that for the PI = 0 silt, the maximum shear strain required to develop large excess pore pressures for repeated loading at the same CSR may be largely independent of the initial fabric. For max $r_u$ values exceeding 75%, increased dilatancy from accumulated reconsolidation strains (0.9% to 1.3% per reconsolidation stage for this specimen) decreased the rate of max shear strain development across the four cyclic shearing stages. It is evident from the responses from DSScsh tests on initially overconsolidated PI = 0 silt specimens that increases in cyclic strength from initial overconsolidation are primarily attributable to fabric and lateral stress effects. Destruction of fabric as well as reduction of lateral earth pressures are most likely responsible for the observed strength loss following cyclic shearing and reconsolidation of initially overconsolidated specimens.

The cyclic strength evolution with prior strain history of initially overconsolidated PI = 0 silt specimens followed the CRR-e trend for initially normally consolidated specimens after the fabric and lateral stresses induced by overconsolidation were functionally erased by the development of large shear strains during cyclic shearing. The progression of cyclic strength with void ratio for three DSScsh tests on initially overconsolidated specimens are shown in Fig. 11. The cyclic strengths of the initially overconsolidated specimens first decrease following cyclic shearing and reconsolidation and then closely follows the CRR-e trend developed for initially normally consolidated specimens in all subsequent cyclic loading stages. The strength evolution following the first cyclic shearing and reconsolidation stages appears to be independent of initial consolidation history, depending on only specimen density, evolving fabric from cyclic shearing, and potential specimen non-uniformities. In addition to consolidation history, other phenomena affecting behavior of natural soils such as ageing, cementation, and biogeochemical processes may develop a soil structure that is similarly prone to strength loss following the development of large shear strains during a single stage of cyclic loading.

**Cyclic Strength Evolution with Prior Strain History for PI = 6 Silt**

The evolution of cyclic strength with prior strain history was evaluated for initially normally consolidated and overconsolidated specimens of the PI = 6 silt following a similar testing program presented for the PI = 0 silt. DSScsh tests were performed on initially normally consolidated specimens with CSRs ramped in stages from 0.12 to 0.6. Reconsolidation strains were of comparable magnitude to those measured for the PI = 0 silt ranging from about 1.6% to 0.3%, decreasing with increasing specimen density. An attempt was made to quantify potential specimen non-uniformities at the end of a DSScsh test on the PI = 6 silt by measuring local water contents of specimen quadrants defined by one vertical and one horizontal cut; no measurable non-uniformities were evident on the scale resolved from this analysis. Results from DSScsh tests on the PI = 6 silt are presented and compared to results for the PI = 0 silt in this section.

The progression of cyclic shearing responses in DSScsh tests on initially normally consolidated specimens was similar for the PI = 0 and PI = 6 silts. Cyclic shearing and reconsolidation responses for four stages (A1, A2, B3, and C4) from a DSScsh test on an initially normally consolidated PI = 6 silt specimen are shown in Fig. 12. Cyclic shearing stages A2, B3, and C4 developed 3% shear strain in close to 15 cycles for CSRs of 0.12, 0.21 and 0.39 respectively; these stages are analogous to the last three stages shown in Fig. 6 for a PI = 0 silt specimen. The responses of these three cyclic shearing stages were similar to the responses of the PI = 0 silt for states of comparable strengths (stages A4, B3 and C2 in Fig 6.). The virgin responses of the two silts (A1 stages in Figs. 6 and 12) were slightly different despite similar strengths. The virgin response of the PI = 6 silt included the development of 3% shear stain at a max $r_u$ of about 90%, such that it did not exhibit the transient near-zero tangent stiffness associated with $r_u$ values approaching 100% in the virgin PI =0 silt response. Like the PI = 0 silt, increased dilatancy from accumulated reconsolidation strains was the primary mechanism of cyclic strength increase for initially normally consolidated specimens of the PI = 6 silt. A similar transition from “loose” states characterized by the development of large shear strains in a few cycles of loading once high excess pore pressures were generated to "dense" states distinguished by gradual large strain accumulation is evident in the test results for both silts.

The strength gain induced by overconsolidation of the PI = 6 silt was similar to that for PI = 0 silt. Overconsolidation to an OCR = 2 caused the PI = 6 silt to develop about 3% volumetric strain relative to a $\sigma'_{vc}$ = 100 kPa normally consolidated reference condition, whereas the PI = 0 silt only developed about 0.5% to 1% volumetric strain. However, post cyclic reconsolidation strains for the two silts are similar at about 1.5-0.3 %, decreasing with decreased void ratio. Despite differences in virgin compressibility, the gains in cyclic resistance from overconsolidation of PI = 6 silt specimens appeared to be functionally destroyed following cyclic shearing and reconsolidation in the same way evident in the PI = 0 silt. The evolution of cyclic shearing response for an initially overconsolidated specimen (OCR = 2) of PI = 6 silt is shown in Fig. 13 for four consecutive cyclic shearing stages at a constant CSR of about 0.19 (stress-strain responses and stress paths are only shown for the first two stages in Figs 13a and 13b). The virgin overconsolidated specimen experienced gradual excess pore pressure generation followed by large shear strain accumulation in a few cycles once the max $r_u$ reaches about 70% (the circles in Fig 13c and 13d correspond to max $r_u$ values of 70%). The virgin overconsolidated pattern of shear strain development is similar to the behavior of the virgin overconsolidated PI = 0 silt, with the generation of excess pore pressure plateauing at an $r_u$ of about 90% for both specimens. Other tests on virgin overconsolidated specimens of PI = 6 silt showed $r_u$ plateauing between 75% and 90%, even though they had consistent cyclic strengths for the failure criteria examined herein. Like the PI = 0 silt, the increased initial rate of pore pressure generation in the subsequent cyclic shearing stages for the initially overconsolidated PI = 6 specimen implies some destruction of the fabric and lateral stresses induced by overconsolidation. Volumetric strains, fabric, and lateral stresses developed from virgin consolidation and post cyclic reconsolidation may be different for the PI = 6 and 0 silt; these differences may be more evident for specimens that are initially further overconsolidated (e.g., specimens with an initial OCR = 4, for which the virgin cyclic strengths shown in Fig. 4 generally exhibited smaller plateauing $r_u$ values).

The progression of cyclic strength for specimens of the PI = 6 silt with the prior strain history imposed by DSScsh testing followed the general pattern exhibited by the PI = 0 silt. Cyclic strengths are plotted versus void ratio in Fig. 14 for DSScsh test on two initially normally consolidated and two initially overconsolidated (OCR =2) specimens of the PI = 6 silt. To project the measured responses from DSScsh tests, the CRR-b relationship adopted from Boulanger and Idris (2014) was shifted to honor the measured b value (0.121) for virgin normally consolidated specimens. Projected cyclic strengths for two data points where the number of loading cycles is less than 4 are plotted for the initially overconsolidated tests to illustrate the approximate strength decrease following the first stages of cyclic shearing and reconsolidation. Data points in Fig. 14 are only plotted for a 3% single amplitude shear strain failure criteria for clarity; the trend for a 5% double amplitude shear strain failure criterion was not significantly different. The CRR-e relationships for the initially normally consolidated PI = 6 specimens follow the derived trends for initially normally consolidated PI = 0 silt specimens at lower CRR values. At a CRR of about 0.3, the PI = 0 and 6 relationships begin to deviate slightly; the PI = 6 silt developed less strength increase per decrease in void ratio than the PI = 0 silt. Further densification, and therefore more stages of cyclic shearing and reconsolidation (the per stage reconsolidation strain magnitudes for the two silts are comparable), were required to reach cyclic strengths exceeding 0.3. This difference in responses seems reasonable given the two silts have similar void ratios when normally consolidated at $\sigma'_v$ =100 kPa (the PI = 6 silt specimens have about a 0.02 greater initial void ratio) and the virgin PI = 0 silt specimens were initially dense of critical state whereas the virgin PI =6 silt specimens were initially loose of critical state (i.e., the critical state line for the PI = 6 silt is lower than for the PI = 0 silt at this value of $\sigma'_v$). It follows that the state (or state parameter) of the PI = 6 silt will continue to be "looser" relative to critical state than the PI = 0 silt at the same void ratio throughout DSScsh testing. Following cyclic shearing and reconsolidation of initially overconsolidated specimens of the PI = 6 silt, the cyclic strength evolution followed the same progression with void ratio experienced by initially normally consolidated specimens for the range of CSRs applied.

**Limitations and Practical Implications**

The effect of multiple earthquake events on liquefaction resistance in the field is likely to vary with several factors not accounted for by laboratory elements tests like those presented herein. For example, it is hypothesized that the fabric developed during uniform uni-directional cyclic DSS testing is likely more pronounced than what develops in situ during three-dimensional irregular cyclic loading, such that the subsequent dependence of cyclic resistance on load directionality is likely more pronounced in laboratory tests than in situ. The drainage conditions during and after shaking in situ can result in non-uniform volumetric strains, including zones of possible loosening beneath lower permeability layers that impede water flow (e.g., void redistribution). Non-uniform volumetric strains could produce non-uniform changes in liquefaction resistance within a deposit, such that the net effect on a site's potential for liquefaction-induced ground deformations could be difficult to predict. Furthermore, the liquefaction resistance of natural soil deposits is known to depend on factors such as age, cementation, and products of biogeochemical processes, which are not recreated in the time frame of laboratory element tests.

The results of these laboratory tests, despite their differences from in-situ environments, offer several insights into the effects of prior strain history on cyclic resistance and provide a basis for understanding such effects for a wider range of soil types and initial conditions. High cyclic strengths, CRRs exceeding 0.6, were developed in both of the silts tested through densification from accumulated post-cyclic reconsolidation strains resulting from multiple cyclic shearing events, suggesting that large cyclic strengths can progressively develop in situ from repeated earthquake shaking events over geologic time. The strength increases associated with single events were, however, relatively modest and consistent with centrifuge test observations by Darby et al. (2016) and El-Sekelley et al. (2016) for sands. The cyclic strength increase per event was smallest for looser sands and greater for dense sands. A loss of cyclic strength from single events is possible if fabric from small strain preshearing, cementation, ageing, biological activity, or consolidation history is damaged during cyclic loading. Loose soils are likely most sensitive to this type of strength loss because of the minimal strength increase associated with post-cyclic densification from single cyclic loading events. Recognizing the potential for strength loss or gain following a liquefaction event may be important for understanding field observations from earthquake sequences or events with significant aftershocks. For in-situ remediation, increases in cyclic strength by densification are likely to have more permanence than by equivalent preloading. The two silts tested demonstrated similar progressions of behaviors with prior strain history despite their differences in plasticity, compressibility, and initial state. The similarity of responses for these two silts and their consistency with trends reported for sands in the literature suggests such responses are likely qualitatively similar for a broad range of liquefiable soils.

## Summary and Conclusions

The evolution of cyclic resistance with multiple cyclic loading and reconsolidation stages for a non-plastic, PI =0 silt and a low plasticity, PI = 6 silt was evaluated using DSScsh testing on slurry deposited specimens. Cyclic shearing stages and reconsolidation stages were repeated until specimens had CRRs exceeding 0.6. Reconsolidation strains of 1.6% to 0.3%, progressively decreasing with increasing density, were observed for both silts. The effect of single cyclic loading events and the cumulative effect of a series of events were examined.

The progression of cyclic strength with prior strain history of the non-plastic, PI = 0 and low plasticity, PI = 6 silts was dependent on initial over-consolidation ratio (OCR), void ratio, failure criterion, and loading directionality. Initially normally consolidated specimens of both silts developed progressive increases in cyclic strength with prior strain history with CRRs ultimately exceeding 0.6; the per event strength increases were initially modest, but became progressively greater as the specimens became denser. Initially over-consolidated specimens with an OCR of 2 had an 18-32% loss of cyclic strength following the first stage of cyclic shearing and reconsolidation, which was attributed to a disruption of the fabric and lateral stresses induced during over-consolidation. The evolution of cyclic shearing responses with prior strain history was similar for the two silts and consistent with trends for sands in the literature. The PI = 0 and 6 silts developed similar magnitudes of reconsolidation strain for similar levels of peak shear strain during undrained cyclic loading. The PI = 6 silt required more volumetric strain (and therefore more events) to develop large cyclic strengths (e.g., above 0.3) than the PI = 0 silt.

The result of the experiments performed in this study are limited to young uncemented non-plastic and low plasticity silts where multiple cyclic loading events occur over a short period of time. In-situ behavior of natural deposits is complicated by many factors not explicitly considered in this study including ageing, cementation, biological activity, and complex loading and drainage conditions. In addition, non-uniformities of strain and density within DSScsh specimens are expected to have influenced the test results. Nonetheless, it is hoped that the results from this study contribute to an improved understanding of the effect of prior strain history on cyclic strength and behavior of silts.

## Acknowledgments

Portions of the work presented herein were derived from studies supported by the California Department of Water Resources (contract 4600009751) and the National Science Foundation (grants CMMI-1138203 and CMMI-1300518). Any opinions, findings, or recommendations expressed in this material are those of the authors and should not be interpreted as necessarily representing the official policies, either expressed or implied, of either organization. Ana Maria Parra Bastidas performed the one-dimensional compression tests presented herein. The authors are grateful for the above assistance and support.

## References

Bjerrum, L., and Landva, A. (1966). "Direct simple-shear tests on a Norwegian quick clay." *Géotechnique*, 16(1), 1-20.

Boulanger, R. W., and Idriss, I. M. (2014). "CPT and SPT based liquefaction triggering procedures." *Rep. No. UCD/CGM-14/01*, Univ. of California, Davis, CA, 134 pp.

Boulanger, R. W., and Idriss, I. M. (2016). "CPT-based liquefaction triggering procedure." *Journal of Geotechnical and Geoenvironmental Engineering*, 142(2), 04015065.

Boulanger, R. W., and Seed, R. B. (1995). "Liquefaction of sand under bidirectional monotonic and cyclic loading." *Journal of Geotechnical Engineering*, 121(12), 870-878.

Bray, J. D., and Sancio, R. B. (2006). "Assessment of the liquefaction susceptibility of fine-grained soils." *Journal of Geotechnical and Geoenvironmental Engineering*, 132(9), 1165-1177.

Castro, G. (1975). "Liquefaction and cyclic mobility of saturated sands, *J. Geotechnical Eng. Div.*, 101(GT6), 551-569.

Darby, K. M., Bronner, J. D., Parra Bastidas, A. M., Boulanger, R. W., and DeJong, J. T. (2016). "Effect of shaking history on cone penetration resistance and cyclic strength of saturated sand." Proceedings, Geotechnical and Structural Engineering Congress, ASCE, Phoenix, AZ, February 14-17.

El-Sekelly, W., Dobry, R., Abdoun, T., and Steidl, J. H. (2016). "Centrifuge modeling of the effect of preshaking on the liquefaction resistance of silty sand deposits." *Journal of Geotechnical and Geoenvironmental Engineering*, 04016012.

Finn, W.D. Liam, L. Bransby and D.J. Pickering (1970). "Effect of Strain History on Liquefaction of Sand", Jour. Of the Soil Mech. And Found. Div., ASCE, 96(SM6), Proc. Paper 7670, 1917-1934

Franke, E., Kiekbusch, M., and Schuppener, B. (1979). "A new direct simple shear device." *Geotechnical Testing Journal*, 2(4), 190-199.

Guo, T., and Prakash, S. (1999). "Liquefaction of silts and silt-clay mixtures." *Journal of Geotechnical and Geoenvironmental Engineering*, 125(8), 706-710.

Ha, I. S., Olson, S. M., Seo, M. W., and Kim, M. M. (2011). "Evaluation of reliquefaction resistance using shaking table tests." *Soil Dynamics and Earthquake Engineering*, 31(4), 682-691.

Hayati, H., and Andrus, R. D. (2009). "Updated liquefaction resistance correction factors for aged sands." *Journal of Geotechnical and Geoenvironmental Engineering*, 135(11), 1683-1692.

Ishihara, K., and Okada, S. (1978). "Effects of stress history on cyclic behavior of sand." *Soils and Foundations*, 18(4), 31-45.

Ishihara, K., and Yoshimine, M. (1992). "Evaluation of settlements in sand deposits following liquefaction during earthquakes." *Soils and Foundations*, 32(1), 173-188.

Ishihara, K. (1993). "Liquefaction and flow failure during earthquakes." *Géotechnique*, 43(3), 351-451.

Kokusho, T., Ito, F., Nagao, Y., and Green, A. R. (2012). "Influence of non/low-plastic fines and associated aging effects on liquefaction resistance." *Journal of Geotechnical and Geoenvironmental Engineering*, 138(6), 747-756.

Maurer, B. W., Green, R. A., Bradley, B. A., and Cubrinovski, M. (2014). "Assessment of aging correction factors for liquefaction resistance at sites of recurrent liquefaction." *10th US National Conference on Earthquake Engineering (NCEE10),* Anchorage, AK, USA.

Mitchell, J.K., and Soga, K. (2005). *Fundamentals of soil behavior*, Wiley, New York.

Oda, M., Kawamoto, K., Suzuki, K., Fujimori, H., and Sato, M. (2001). "Microstructural interpretation on reliquefaction of saturated granular soils under cyclic loading." *J. Geotech. and Geoenviron. Eng.*, 127(5), 416-423.

Olson, S. M., Obermeier, S. F., and Stark, T. D. (2001). "Interpretation of penetration resistance for back-analysis at sites of previous liquefaction." *Seismological Research Letters*, 72(1), 46-59.

Romero, S. (1995). *The behavior of silt as clay content is increased*. MS thesis, University of California, Davis, 108 pp.

Sanin, M. V., and Wijewickreme, D. (2006). "Cyclic shear response of channel-fill Fraser River Delta silt." *Soil Dynamics and Earthquake Engineering*, 26(9), 854-869.

Seed, H. B., Chan, C. K., and Mori, K. (1977). "Influence of seismic history on liquefaction of sands." *J. Geotech. Eng. Div.,* ASCE, 103(4), 257-270.

Suzuki, T., and Toki, S. (1984). "Effects of preshearing on liquefaction characteristics of saturated sand subjected to cyclic loading." *Soils and Foundations*, 24(2), 16-28.

Wakamatsu, K. "Recurrent liquefaction induced by the 2011 Great East Japan earthquake compared with the 1987 earthquake." *Proc., The International Symposium on Engineering Lessons Learned from the 2011 Great East Japan Earthquake*, 675-686.

Wijewickreme, D., and Soysa, A. (2016). "Stress–strain pattern–based criterion to assess cyclic shear resistance of soil from laboratory element tests." *Canadian Geotechnical Journal*, 53(9), 1460-1473.

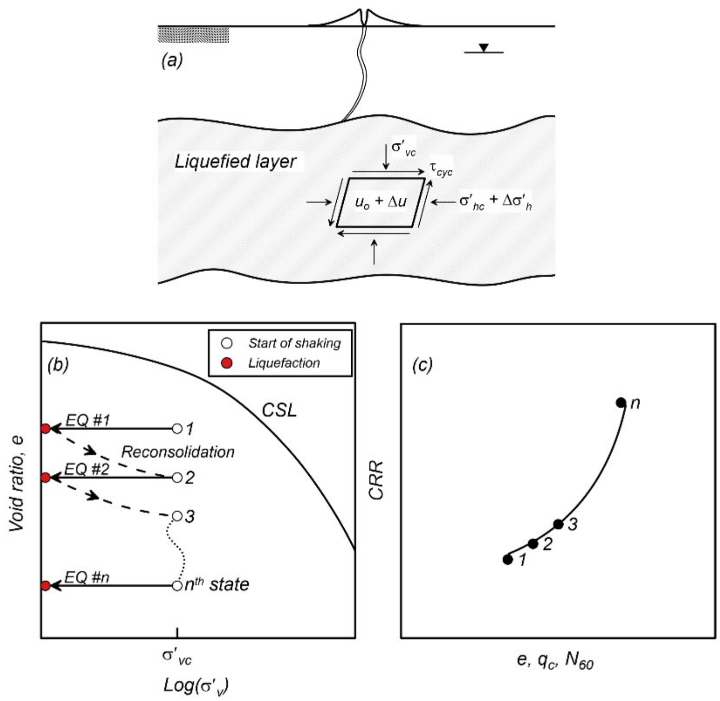

(a)
Liquefied layer
σ'vc
τcyc
uo + Δu
σ'hc + Δσ'h
(b)
Start of shaking
Liquefaction
CSL
EQ #1
1
Reconsolidation
EQ #2
2
3
EQ #n
nth state
Void ratio, e
σ'vc
Log(σ'v)
(c)
n
3
2
1
CRR
e, qc, N60

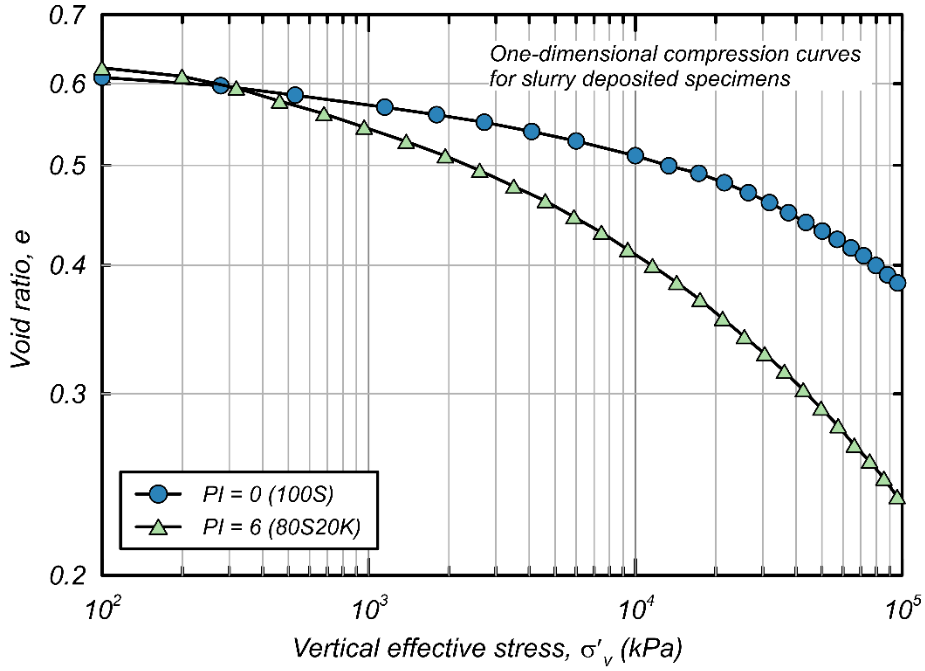

One-dimensional compression curves
for slurry deposited specimens
PI = 0 (100S)
PI = 6 (80S20K)
Void ratio, e
0.7
0.6
0.5
0.4
0.3
0.2
10^2
10^3
10^4
10^5
Vertical effective stress, σ'v (kPa)

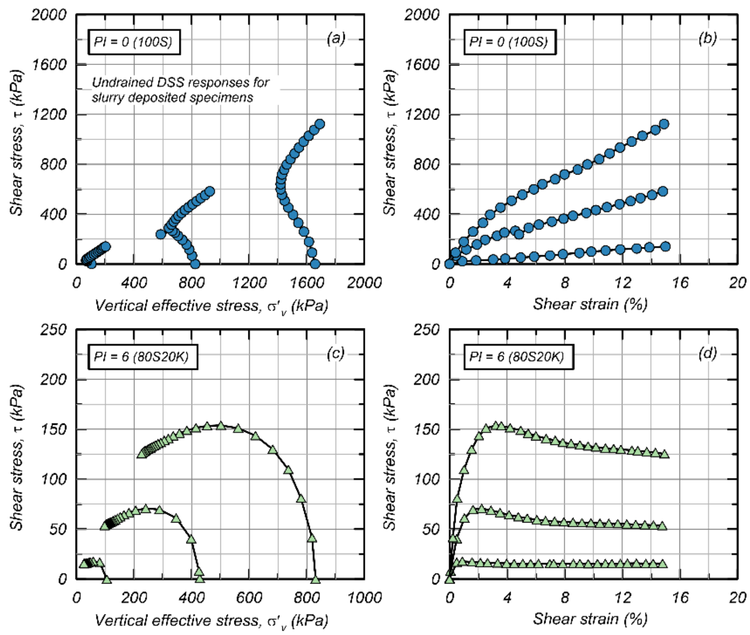

PI = 0 (100S)
(a)
Undrained DSS responses for slurry deposited specimens
Shear stress, τ (kPa)
Vertical effective stress, σ'v (kPa)
PI = 0 (100S)
(b)
Shear stress, τ (kPa)
Shear strain (%)
PI = 6 (80S20K)
(c)
Shear stress, τ (kPa)
Vertical effective stress, σ'v (kPa)
PI = 6 (80S20K)
(d)
Shear stress, τ (kPa)
Shear strain (%)

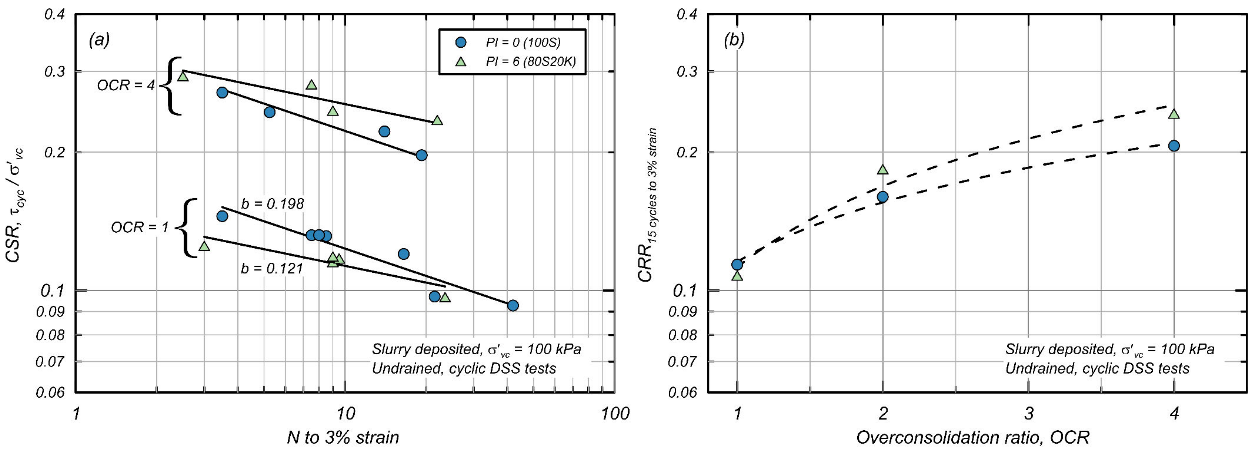

(a)
PI = 0 (100S)
PI = 6 (80S20K)
OCR = 4
OCR = 1
b = 0.198
b = 0.121
CSR, $\tau_{cyc}$ / $\sigma'_{vc}$
N to 3% strain
Slurry deposited, $\sigma'_{vc}$ = 100 kPa
Undrained, cyclic DSS tests
(b)
$CRR_{15\ cycles\ to\ 3\%\ strain}$
Overconsolidation ratio, OCR
Slurry deposited, $\sigma'_{vc}$ = 100 kPa
Undrained, cyclic DSS tests

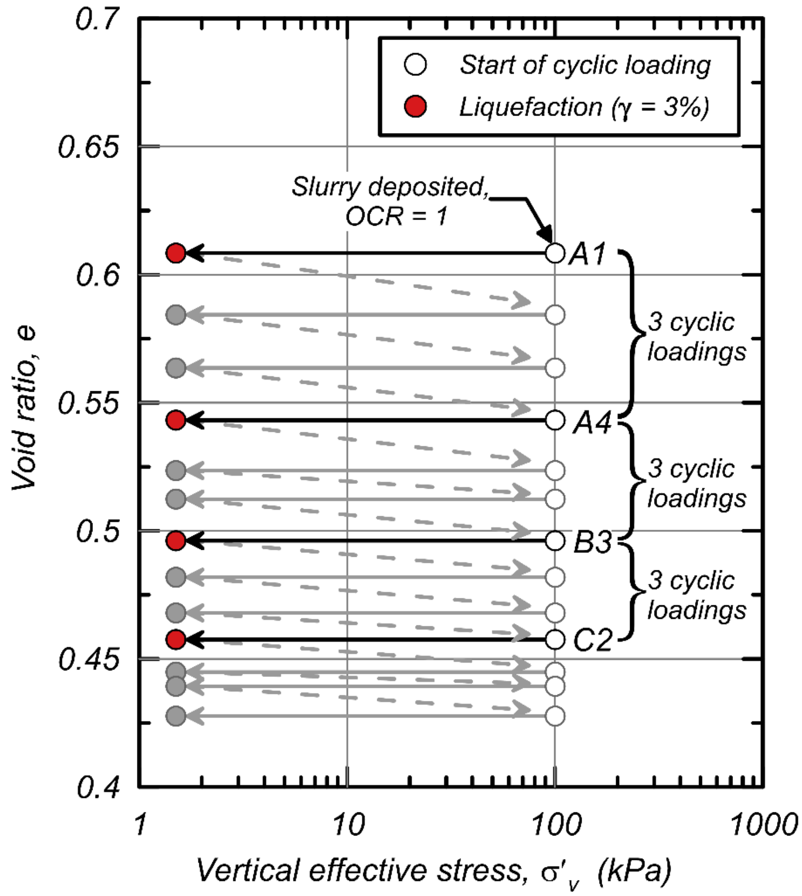

0.7
0.65
0.6
0.55
0.5
0.45
0.4
Void ratio, e
1
10
100
1000
Vertical effective stress, σ'v (kPa)
Start of cyclic loading
Liquefaction (γ = 3%)
Slurry deposited,
OCR = 1
A1
A4
B3
C2
3 cyclic loadings
3 cyclic loadings
3 cyclic loadings

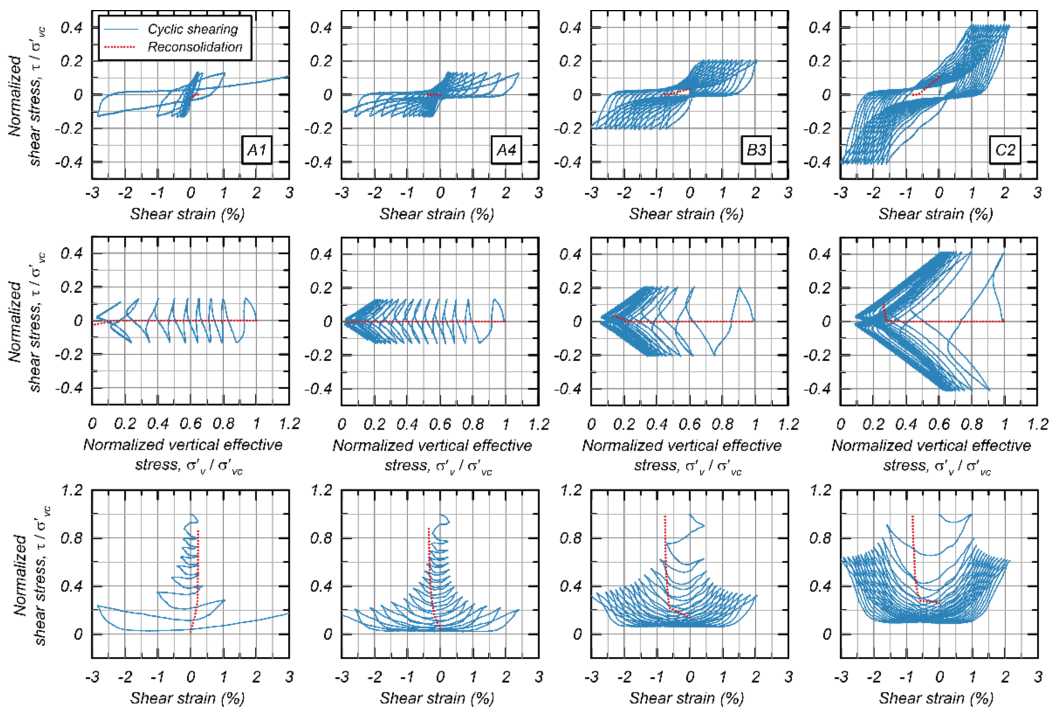

Cyclic shearing
Reconsolidation
A1
A4
B3
C2
Normalized shear stress, τ / σ'vc
Shear strain (%)
Normalized vertical effective stress, σ'v / σ'vc

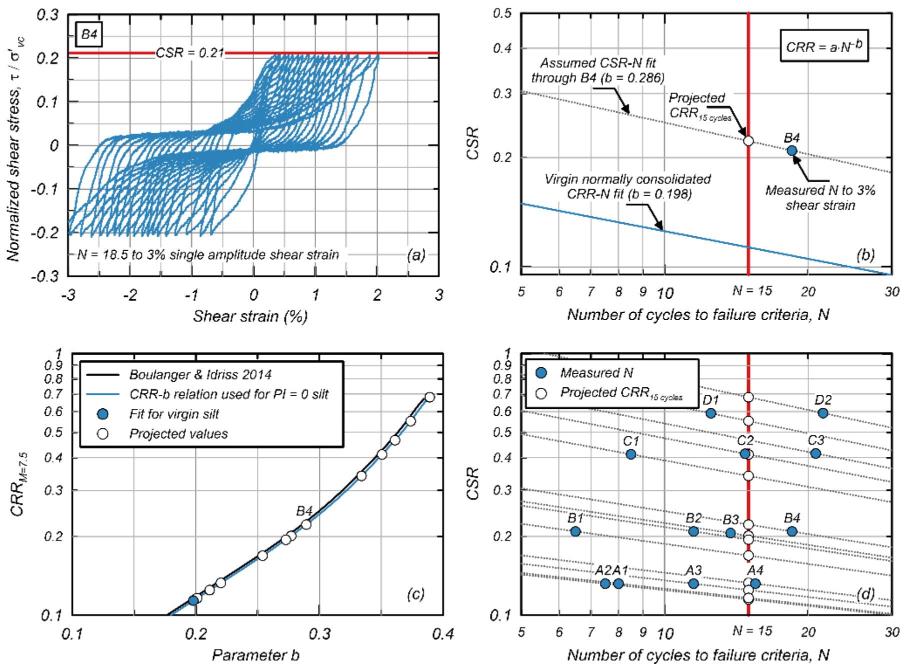

B4
CSR = 0.21
N = 18.5 to 3% single amplitude shear strain
(a)
Normalized shear stress, τ / σ'vc
Shear strain (%)
CRR = a·N^-b
Assumed CSR-N fit through B4 (b = 0.286)
Projected CRR15 cycles
B4
Measured N to 3% shear strain
Virgin normally consolidated CRR-N fit (b = 0.198)
(b)
CSR
N = 15
Number of cycles to failure criteria, N
Boulanger & Idriss 2014
CRR-b relation used for PI = 0 silt
Fit for virgin silt
Projected values
B4
(c)
CRRM=7.5
Parameter b
Measured N
Projected CRR15 cycles
D1
D2
C1
C2
C3
B1
B2
B3
B4
A2
A1
A3
A4
(d)
CSR
N = 15
Number of cycles to failure criteria, N

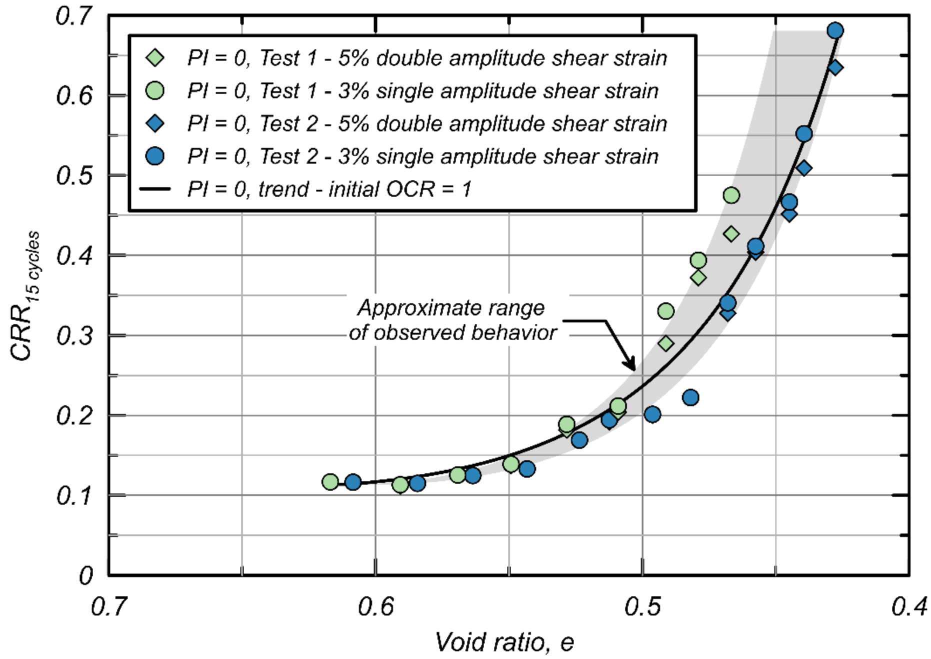

PI = 0, Test 1 - 5% double amplitude shear strain
PI = 0, Test 1 - 3% single amplitude shear strain
PI = 0, Test 2 - 5% double amplitude shear strain
PI = 0, Test 2 - 3% single amplitude shear strain
PI = 0, trend - initial OCR = 1
Approximate range
of observed behavior
CRR15 cycles
Void ratio, e
0.7
0.6
0.5
0.4
0.3
0.2
0.1
0
0.7
0.6
0.5
0.4

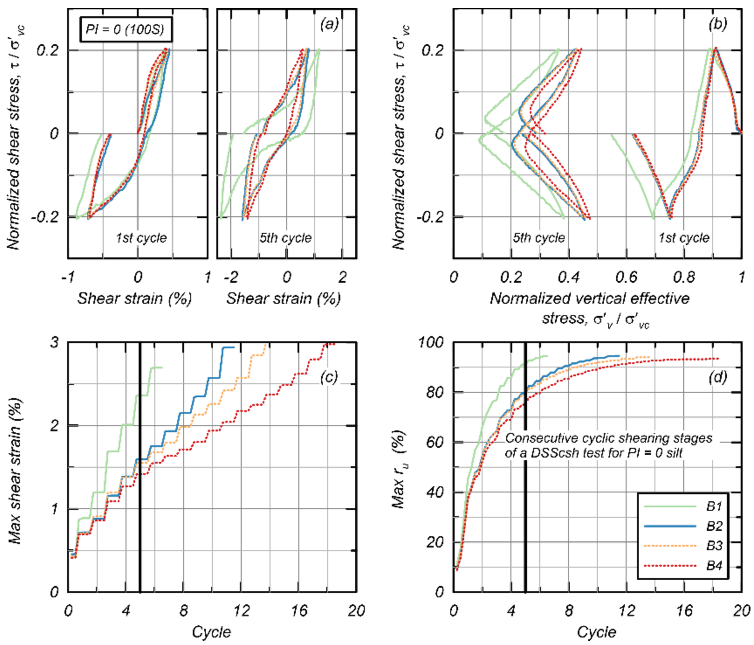

PI = 0 (100S)
(a)
(b)
(c)
(d)
Normalized shear stress, τ / σ'vc
0.2
0
-0.2
1st cycle
5th cycle
-1
0
1
-2
0
2
Shear strain (%)
Shear strain (%)
0
0.2
0.4
0.6
0.8
1
Normalized vertical effective stress, σ'v / σ'vc
Max shear strain (%)
3
2
1
0
0
4
8
12
16
20
Cycle
Max ru (%)
100
80
60
40
20
0
Consecutive cyclic shearing stages of a DSScsh test for PI = 0 silt
B1
B2
B3
B4

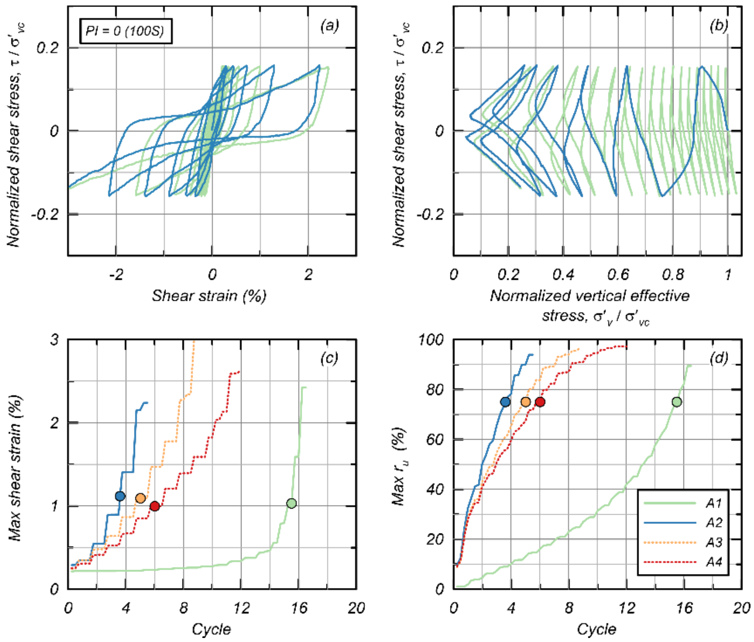

PI = 0 (100S)
(a)
(b)
(c)
(d)
Normalized shear stress, τ / σ'vc
Shear strain (%)
Normalized vertical effective stress, σ'v / σ'vc
Max shear strain (%)
Max ru (%)
Cycle
A1
A2
A3
A4

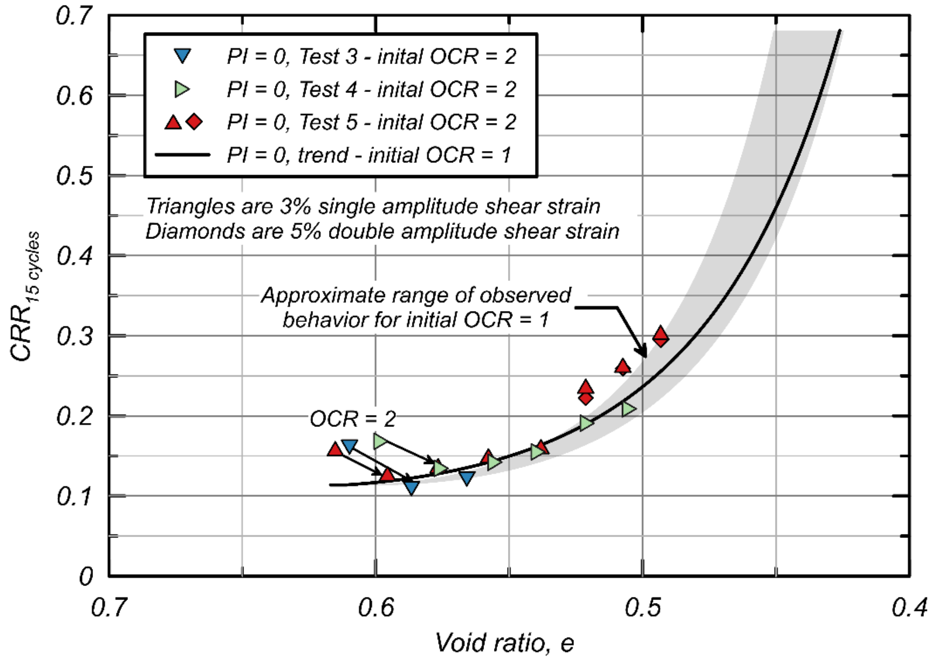

PI = 0, Test 3 - inital OCR = 2
PI = 0, Test 4 - inital OCR = 2
PI = 0, Test 5 - inital OCR = 2
PI = 0, trend - initial OCR = 1
Triangles are 3% single amplitude shear strain
Diamonds are 5% double amplitude shear strain
Approximate range of observed behavior for initial OCR = 1
OCR = 2
$CRR_{15\ cycles}$
Void ratio, e
0.7
0.6
0.5
0.4
0.3
0.2
0.1
0
0.7
0.6
0.5
0.4

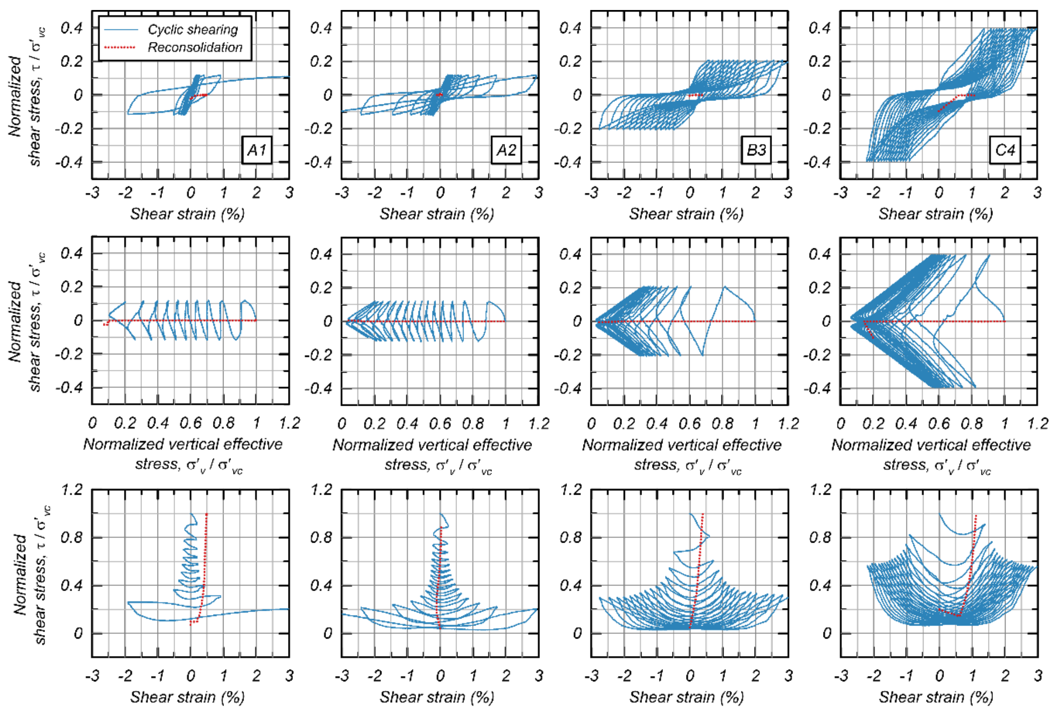
Cyclic shearing
Reconsolidation
A1
A2
B3
C4
Normalized shear stress, τ / σ'vc
Shear strain (%)
Normalized vertical effective stress, σ'v / σ'vc
Normalized shear stress, τ / σ'vc

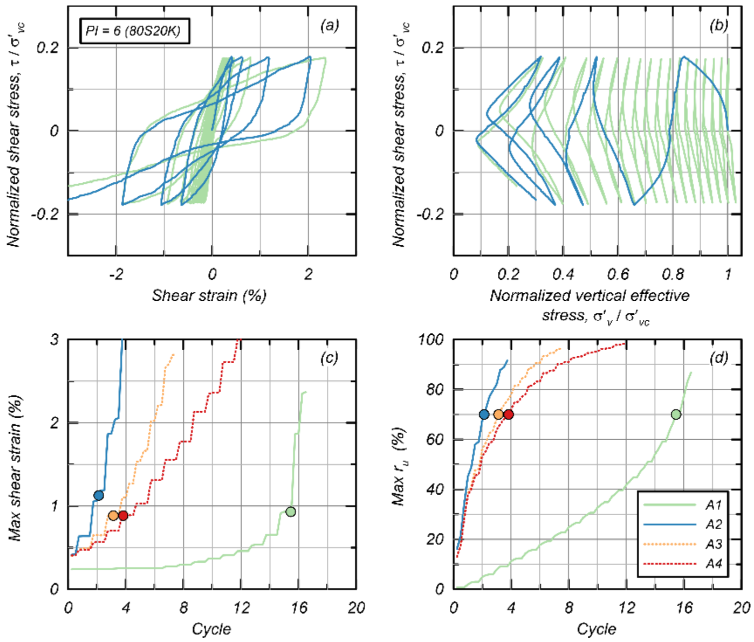
PI = 6 (80S20K)
(a)
Normalized shear stress, τ / σ'vc
Shear strain (%)
(b)
Normalized vertical effective stress, σ'v / σ'vc
(c)
Max shear strain (%)
Cycle
(d)
Max ru (%)
A1
A2
A3
A4

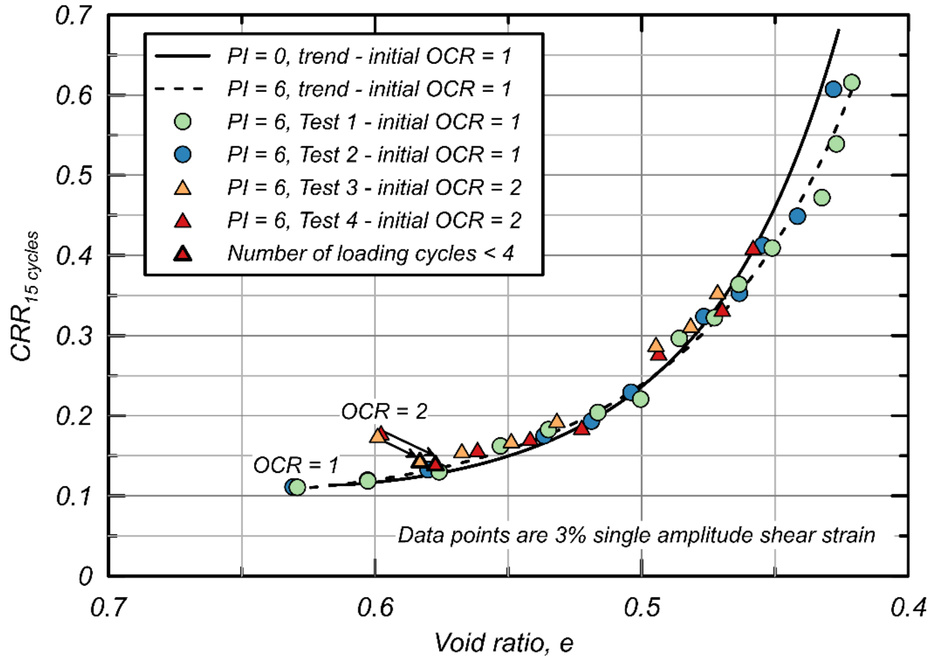

PI = 0, trend - initial OCR = 1
PI = 6, trend - initial OCR = 1
PI = 6, Test 1 - initial OCR = 1
PI = 6, Test 2 - initial OCR = 1
PI = 6, Test 3 - initial OCR = 2
PI = 6, Test 4 - initial OCR = 2
Number of loading cycles < 4
OCR = 2
OCR = 1
Data points are 3% single amplitude shear strain
$CRR_{15\ cycles}$
Void ratio, e
0.7
0.6
0.5
0.4
0.3
0.2
0.1
0
0.7
0.6
0.5
0.4